Food Bioprocess Technol (2014) 7:2472–2483
DOI 10.1007/s11947-014-1256-3

ORIGINAL PAPER

Peptide Microencapsulation by Core–Shell Printing Technology for Edible Film Application

N. Blanco-Pascual · R. B. J. Koldeweij · R. S. A. Stevens · M. P. Montero · M. C. Gómez-Guillén · A. T. Ten Cate

Received: 4 August 2013 / Accepted: 6 January 2014 / Published online: 18 January 2014

Abstract This paper presents a new microencapsulation methodology for incorporation of functional ingredients in edible films. Core–shell microcapsules filled with demineralized water (C) or 1 % (w/v) peptide solution (Cp) were prepared using the microencapsulation printer technology. Shell material, composed of a stearic acid/carnauba wax mixture (75:25), represented around 10 % of the capsule weight, corresponding to a shell material/peptide ratio of 13.3:1 on dry basis. C capsules were more spherical and homogeneous than Cp ones. Cp's more irregular morphology would explain the slightly higher size of d_{90} (126 μm) compared to C (122.50 μm). Cp microcapsules were more stable at pH 5 and 7 (<30 % peptide released in 3 h) than at pH 2 and 9.2 (40–50 % released in 3 h). A procedure for homogeneous microencapsule inclusion in hydrophilic *Laminaria digitata* edible films was developed, without losing microcapsule integrity either in the filmogenic solution or during the drying process. Films with added microcapsules were stronger and more deformable, more opaque, more water-soluble but less permeable to water vapour and less resistant to perforation.

Keywords Microencapsulation · Inkjet printing · *Laminaria digitata* · Edible film · Stability · Release

This centre has implemented and maintains a Quality Management System which fulfils the requirements of the ISO standard 9001:2000

N. Blanco-Pascual · M. P. Montero · M. C. Gómez-Guillén (✉)
Instituto de Ciencia y Tecnología de Alimentos y Nutrición (ICTAN-CSIC), C/ José Antonio Nováis, 28040 Madrid, Spain
e-mail: cgomez@ictan.csic.es

R. B. J. Koldeweij · R. S. A. Stevens · A. T. T. Cate
Netherlands Organization for Applied Scientific Research (TNO), PO Box 6235, 5600 HE Eindhoven, The Netherlands

Introduction

Microcapsules have been widely developed in food industry and used as carriers of different substances for a range of applications, such as core material protection or controlled delivery systems (Gibbs et al. 1999). The most commonly used encapsulation techniques are emulsification, coacervation, spray drying, spray cooling, freeze drying, fluid bed coating and extrusion technologies, liposome and cyclodextrin encapsulation (de Vos et al. 2010; Gibbs et al. 1999). A relatively new approach for the preparation of well-defined core–shell microcapsules is the TNO encapsulation printer (Houben 2012), which has never before been reported to be used in food applications.

Core–shell microcapsules have the advantage that they allow high payloads and well-defined release characteristics, in contrast to matrix-type microcapsules as, for instance, prepared by spray-drying (Gouin, 2004). However, core–shell capsules are often more difficult to produce. Encapsulation printing is a suitable technique to prepare high quality monodisperse core–shell microcapsules. Compared to, for instance, coacervation methods, this technique presents advantages such as the continuity and the mildness of the process, and the wide range of materials that can be processed (aqueous, oils/waxes, polymers, solutions, dispersions).

There are many natural and synthetic polymers used for microcapsule preparation, and there are a number of advantages related to lipid materials for their use as matrix agents, like their biocompatibility, biodegradability, ability to entrap a wide range of water soluble and insoluble compounds and the fact that they are also fairly economic (Bhoyar et al. 2011). Carnauba wax is a thermoplastic solid obtained from the carnauba plant tree, consisting of a complex mixture of high molecular weight esters of acids and hydroxyacids that combined with stearic fatty acid forms water resistant structures at room temperature which melt at elevated temperatures (over

69.6°C for stearic acid and 82–86°C for carnauba wax). Carnauba wax/stearic acid combination has shown good results in previous different types of encapsulation studies (Fini et al. 2011; Balducci et al. 2011) being potentially suitable for the microencapsulation printer process due to its matrix characteristics.

Protein encapsulation by organic matter has been previously stated to preserve the activity of protein material both in dry and wet basis (Gibbs et al. 1999; Tomaszewski et al. 2011). The development of a lipid-based microencapsulation method is an interesting approach to preserve potentially active ingredients, such as peptides or polyphenols, or even enhance their efficacy (Goodwin et al. 2012) for different food applications, while masking undesired properties such as the typically bitter peptide flavour (Sun-Waterhouse and Wadhwa 2013) and excessive plasticizer effect (Giménez et al. 2009).

Renewable and biodegradable biopolymers have been widely investigated as edible film materials (Krochta and DeMulderJohnston 1997). Polymers derived from underused natural resources, such as seaweeds, offer the greatest opportunities since their environmental compatibility is assured. Full extraction of *Laminaria digitata* seaweed may advantageously use the distinct functional characteristics of each film-forming ingredient like alginates, proteins and minerals. Proteins and polysaccharides normally form films with good mechanical properties but poor water barriers, because of their hydrophilicity, and lipid-nature microcapsule incorporation might improve their qualities. Although polysaccharides have been previously used for encapsulating lipid phases or emulsions and related applications (Balducci et al. 2011), no information exists in the literature on the film-forming consequences of microcapsule addition to alginate-based *L. digitata* extract as film principal matrix component.

The aims of this paper were (1) to develop a new methodology for microencapsulation of bioactive peptides, (2) to characterize the physical properties and stability of the microcapsules, (3) to investigate the inclusion of microcapsules in alginate-based films and (4) to characterize the structural and physico-chemical properties of the resulting films.

Materials and Methods

Materials

Analytical grade stearic acid and carnauba wax were obtained from Sigma-Aldrich (Zwijndrecht, Netherlands) and glycerol and polysorbate 80 (Tween 80) were obtained from Panreac Química S.A. (Montplet and Esteban S.A., Montcada i Reixac, Barcelona, Spain). The peptide fraction <1 kDa was obtained from dried *Dosidicus gigas* tunics subjected to enzymatic hydrolysis with Esperase (EC 232.752.2; 8.0 l) supplied by Novozymes (Bagsvaerd, Denmark), followed by centrifugal ultrafiltration at 3,000 rpm, 20°C for 15 min (Heraeus Multifuge 3 L-R; Thermo Fisher Scientific, Waltham, MA, USA) with molecular weight cut-off membrane of 1 kDa (Macrosep® Centrifugal Devices; Pall Corporation, Port Washington, NY, USA). The major constituent amino acids, expressed as ‰ residues, were Gly (219), Ala (101), Ser (77), Glu (72), Pro (64), Arg (64), Leu (57) and Asp (54). The composition in total hydrophobic amino acids was 537‰ residues (Mosquera et al., 2013).

Viscosity

The viscosity of the materials used for the encapsulation process was measured using an Anton Paar MCR 301 rheometer with concentric cylinder geometry. Samples were placed in the rheometer, equilibrated at each temperature (35°C for demineralized water and 1 % peptide solution, 105°C for shell material) for 2 min.

Surface Tension and Contact Angle Measurements

The surface tension of the materials used for the encapsulating process was measured using a Krüss contact angle measuring system G10 (Etten-Leur, The Netherlands). Surface energy of liquid droplets was calculated using the static sessile drop method.

Surface hydrophobicity and wettability of the shell material in the filmogenic solution were evaluated from contact angle measurements (static sessile drop method) using a Krüss contact angle measuring system DSA100 at 21±1°C. A droplet (6.04±0.02 μl) of *L. digitata* filmogenic solution at 21±1°C (1.04±0.03 g/ml) was deposited on a thin smooth layer of shell material at 21±1°C with a precision syringe. The method is based on the image processing and curve fitting for contact angle measurement from a theoretical meridian drop profile, measuring contact angle between the baseline of the drop and the tangent at the drop boundary. The contact angle was measured on both sides of the drop and averaged (θ).

Encapsulation Printing Technology

A custom-built set-up was used for microencapsulation printing experiments, consisting of: a heated reservoir for the core fluid connected to a high pressure pump; a heated piezo-driven print-head with a 30-μm-diameter nozzle; a heated reservoir for liquid shell material, connected to a pump system and a splash-plate type nozzle, in which a jet of fluid shell material impinges on a splash plate, resulting in a thin, fluid curtain of shell material (Fig. 1).

Demineralized water and 1 % peptide solution were used as core fluids to prepare C and Cp microcapsules, respectively. A stearic acid and carnauba wax mixture (75:25) was used as

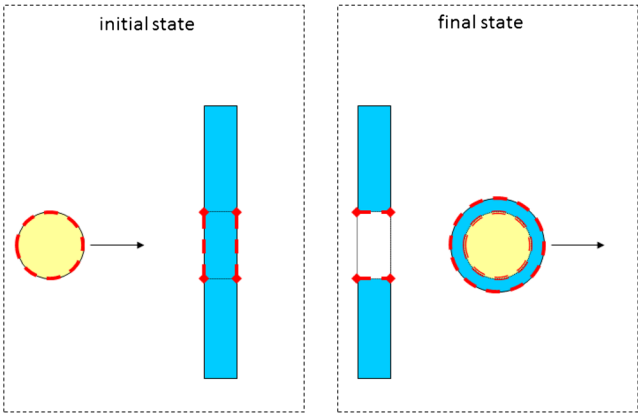

Fig. 1 Schematic of the core material droplet generated by the inkjet technology before and after being printed through the screen made of shell material (Encapsulation of micron sized droplets, RBJ Koldeweij, MSc thesis, University of Twente, 2010)

shell material. Core fluids were printed at 35 °C, at a flow rate of 0.75 ml/min and a frequency of 20 kHz, producing core droplets of 106 μm. The shell material was processed at 105 °C and a flow rate of 29.6 ml/min to produce a thin liquid film over a splash plate at 85°C. Densities of materials were 0.81±0.03 g/ml for shell material at 105°C, 0.97±0.02 g/ml for demineralized water at 35°C and 1.04±0.02 g/ml for 1 % peptide solution at 35°C.

Seaweed Unrefined Extraction

Dried *L. digitata* seaweed (Porto-Muiños, Cerceda, A Coruña, Spain) was homogenized using an Osterizer blender (Oster, Aravaca, Madrid, Spain) with 0.1 M H_2SO_4 solution in 1:10 (w/v) proportion and kept for 12 h at 3±2°C and washed several times with running tap water until stabilizing pH (portable pH-meter series 3 Star Orion with an electrode pH ROSS; Thermo Fisher Scientific, Landsmeer, The Netherlands). Seaweed extraction was carried out with magnetic stirring in 4 % Na_2CO_3 solution at 1:60 (w/v) proportion during 3 h at 75°C, then homogenized in an Osterizer blender and centrifuged at 6,000 rpm for 5 min (Sorvall Evolution RC Centrifuge; Thermo Fisher Scientific, Landsmeer, The Netherlands). In order to remove excess of carbonate salts, the supernatant was dialyzed overnight in 32/32 dialysis tubing (Visking membrane MWCO-12-14000 regenerated cellulose; Medicell International Ltd, London, UK) at 3±2°C. The dialysed supernatant was dried in an oven for 2 days (FD 240 Binder, Tuttlingen, Germany) at 65.0±0.8°C and stored at 21°C until use. The proximate composition of the dried alginate-based extract was ~17 % moisture, 5.5 % protein, ~47 % ash and ~30 % carbohydrate plus other minor compounds (Blanco-Pascual, Montero & Gómez-Guillén, 2014).

Film Preparation

Film-forming solutions were prepared by suspending 3 % w/v dry *L. digitata* unrefined extract in distilled water and homogenizing with magnetic stirring during 15 min at 75°C. Glycerol was added at 0.9 % proportion (w/v) as plasticizer. The pH of the film-forming solutions (FS) was 10±0.4. Microcapsules were added at 1 % (w/v) as dry powder and homogeneously dispersed with a mild magnetic stirring. Surfactant polysorbate 80 was added at 0.1 % (w/v) to help in microcapsules dispersion, and film forming solutions were cast into Petri dishes. Strong microcapsule aggregation still occurred during the film drying process at 35°C. Considering that microcapsules tended to float or migrate to the surface of the biopolymer solution, a porous membrane (TMTP09030 Isopore polycarbonate membranes; Millipore, Billerica, MA, USA) was placed over the solution to immobilize the well dispersed microcapsules in the presence of the surfactant, avoiding aggregation during film drying. Dishes were dried in an oven (FD 240 Binder, Tuttlingen, Germany) at 35.0±0.8°C for 7 h. The polycarbonate membranes were removed from the dried films before conditioning at 58.0±0.2 % RH and 22±1°C for 4 days, prior to analysis. Three types of films were obtained: films with water-filled capsules (F-C), with peptide-filled capsules (F-Cp) and control films without capsules (F).

Differential Scanning Calorimetry (DSC)

Shell material percentage of freshly prepared microcapsules was calculated measuring each enthalpy proportion (ΔH, by linear baseline integration) with respect to the shell material melting enthalpy reference, using a Discovery Series differential scanning calorimeter (TA Instruments, New Castle, DE, USA) previously calibrated.

Calorimetric analysis of F, F-C and F-Cp films were performed using a DSC model TA-Q1000 (TA Instruments) previously calibrated.

For all DSC experiments, samples of around 10–15 mg were weighed and sealed in aluminium hermetic pans. They were scanned under dry nitrogen purge (50 ml/min) between 5°C and 115°C at a heating rate of 10°C/min. Peak temperatures (T_{peak}, °C) and melting enthalpies were measured at least in triplicate and normalized to dry matter content (J/g_{dm}) for film structure analysis.

Laser Scattering Analysis

Particle diameter of the microcapsules was measured using laser scattering analysis (Mastersizer; Malvern Instruments Ltd, Malvern, UK) with a small volume of isopropyl alcohol microcapsule dispersion homogenized in a dispersion unit controller. All the measurements were performed at room temperature with a refractive index of 1.45 and expressed as

volume % of microcapsules. Particle size distribution was expressed in terms of d_{10}, d_{50} and d_{90} (μm), which correspond to the accumulative frequencies of 10 %, 50 % and 90 %, respectively, of particles that are smaller than the indicated size.

Peptide Encapsulation Efficiency and Stability

The peptide entrapment in the microcapsules was determined after total release of the capsule content in distilled water at 95°C during 20 min, in order to melt the lipid shell material. Then, the solution was cooled down to room temperature to precipitate out the lipids and filtered through 0.45-μm pore size filters.

Peptide concentration was determined at 280 nm with the Synergy HT Multi-Mode Microplate Reader and the UV-spectrophotometer Gen5™ BioTek's microplate data collection and analysis software (BioTek Instruments, Inc., Winooski, Vermont, USA). Demineralized water microcapsules results were taken into account as reference due to their small interference in the results caused by a slight release of matrix material (half-order release rate) (Shahidi and Han 1993). Determinations were carried out in triplicate and the mean value of peptide released was calculated using a standard calibration curve made with increasing concentrations of peptide solution (0.1–2 mg/ml).

Peptide encapsulation efficiency was calculated by using the following formula:

Encapsulation efficiency = Peptide entrapped/Theoretical peptide content × 100.

For pH stability studies, microcapsules were placed into different buffer solutions, at pH 2.6, 5 and 7 (citrate–phosphate buffer) and pH 9.2 (carbonate–bicarbonate buffer) at 21 ±1°C and were filtered through 0.45-μm pore size filters after 10 min, 1 h and 3 h, respectively. All samples were evaluated in triplicate.

For film process stability studies, microcapsules were placed either into distilled water (pH 7) or into pH10 aqueous solution (0.012 % Na_2CO_3) at 35±1°C for 30 min, 1 h, 3 h, 5 h, 7 h and 9 h, and were filtered through 0.45-μm pore size filters prior to peptide concentration analysis. All determinations were evaluated in triplicate.

Microcapsule and Film Morphology

Optical microscopy using a Zeiss AxioImager M1m microscope with Epiplan objectives, 100 W Halogen illumination source and AxioCam MRc 5 camera (Zeiss, Sliedrecht, The Netherlands) was used to measure microcapsule diameter and morphology.

Low temperature scanning electron microscopy (LowT-SEM) (Oxford CT1500 Cryosample Preparation Unit, Oxford Instruments, Oxford, England) was used to examine microcapsules and representative film surface and cross sections. Samples were mounted with an optical coherence tomography (OCT compound Gurr ®) and mechanically fixed onto the specimen holder and cryo-fractured after mounted as described by Gómez-Guillén et al. (2007).

Panoramic films pictures were taken with a Canon EOS 550d, MP-E 65 mm optical lens at 5:1 amplification (Canon España, Alcobendas, Madrid, Spain).

Film Characterization

Thickness

Film thickness of F, F-C and F-Cp was measured using a micrometer (MDC-25 M, Mitutoyo, Kanagawa, Japan), averaging the values of six to eight random locations in 15 films for each treatment as described by Perez-Mateos et al. (2009).

Moisture Content

Moisture content of films F, F-C and F-Cp was determined at least in triplicate by drying samples of around 0.5 g at 105 °C for 24 h, according to the AOAC (1995). Water content was expressed as a percentage of total weight.

Optical Properties

The transparency of films F, F-C and F-Cp was calculated at least in triplicate using a UV-1601 spectrophotometer (Model CPS-240; Shimadzu, Kyoto, Japan) at 600 nm following the method described by Perez-Mateos et al. (2009). The films were cut into a rectangular piece and directly placed in the spectrophotometer test cell, using an empty test cell as the reference. Transparency was calculated by the equation, Transparency$=-\log(T_{600}/x)$, where T_{600} is the light transmission (T) at 600 nm and x is the film thickness (mm). According to this equation, higher values would indicate lower degree of transparency.

The colour parameters of lightness (L^*), redness (a^*), and yellowness (b^*) were measured following the method described by Blanco-Pascual et al. (2013).

Water Barrier Properties

Water vapour permeability (WVP) of films F, F-C and F-Cp was determined at least in triplicate following the method described by Sobral et al. (2001) at room temperature and in a dessicator with distilled water.

Film solubility was measured at least in triplicate following the method described by Blanco-Pascual et al. (2013).

Mechanical Properties

Tensile and puncture tests of films F, F-C and F-Cp were run at least in triplicate using a texture analyzer TA.XT plus TA-XT2 (Texture Technologies Corp., Scarsdale, NY, USA) as was described by Blanco-Pascual et al. (2013) but with tensile test samples of 70×20 mm.

Statistical Analysis

One-way analysis of variance was performed using the SPSS computer programme (SPSS Statistical Software Inc., Chicago, IL, USA). The variance homogeneity was made using the Levene test or, the Brown–Forsythe when variance conditions were not fulfilled. Paired comparisons were made using the Bonferroni test or the Tamhane test (depending on variance homogeneity), with the significance of the difference set at $P \leq 0.05$.

Results and Discussion

Encapsulation Printing

Both the viscosity and the surface tension of the starting materials are important parameters in the encapsulation printing process. For the selected nozzle size of 30 μm and flow rate of 0.75 ml/min, the viscosity limit for the core liquids was around 40 mPa s in order to be processable through the inkjet nozzle at reasonable pressure. Shear-rate dependent viscosities of the core fluids were measured at the intended printing temperature (35 °C). The 1 % peptide solution and demineralized water remained fluid with low, shear-independent viscosity values of 0.75–0.82 mPa s up to shear rates of 100 s^{-1} for 1 % peptide solution and 1,000 s^{-1} for demineralized water. Maximum viscosity values at 4,000 s^{-1} were 1.7 mPa s for demineralized water and 7 mPa s for 1 % peptide solution. Shell material viscosity was also low (7–7.6 mPa s) and almost shear-independent at the intended used temperature, which allows formation of a thin liquid curtain to be used for encapsulation. Since in general viscosity values did not increase too much at high shear rates, both shell and core materials were ideal for the encapsulation printing process.

Surface tension values were 32.70±0.13 mN/m for 1 % peptide solution (35°C), 70.20±0.15 mN/m for demineralised water (35°C) and 35.63±0.18 mN/m for the shell material (105°C). Even at this low peptide concentration, surface tension of demineralized water and peptide solution were significantly different, indicating that the peptides act as surfactants, which could affect the process and result in different encapsulation efficiency.

Using the microencapsulation printer, core–shell microcapsules C and Cp were prepared, containing demineralized water or 1 % peptide solution, respectively, inside a lipid shell.

Microcapsule Characterization

Regarding the microcapsules morphology, at the optical microscope (Fig. 2a), microcapsule size was covered between 110 and 140 μm of the diameter. The smallest microcapsules in this range were the expected result, in agreement with the targeted core droplet size of 106 μm, whilst bigger microcapsules might be caused by the collision and coalescence of two core droplets before or during encapsulation. C capsules were somewhat more uniform and spherical than Cp capsules. Overall, the observed capsules did not have cracking or porosity, which suggested high encapsulated materials integrity. There was no microcapsule aggregation, which is one of the main problems in encapsulation techniques, probably due to the carnauba wax presence (Joseph and Venkataram 1995).

At the low temperature-scanning electron microscopy (LT-SEM; Fig. 2b), Cp microcapsules were sometimes more oval-shaped with single protrusions and presumptive peptide material in the surface of some of them, revealing that the microcapsules were not as smooth as C. A small percentage of both C and Cp presented a little circular hole in one of the apices, which probably corresponded to an inefficient closure of the shell material during the encapsulation process, explaining the peptide material presence outside of Cp capsules. Cp irregularities might be caused by a slight interaction between peptides and stearic acid from the shell material. Stearic acid has shown to attract peptides and proteins from aqueous phases (Zadmard and Schrader 2004). A previous LT-SEM study showed smooth and regular carnauba wax microcapsules of similar size and stearic acid microcapsules with fracture lines and irregularities on the surface (Fini et al. 2011), which might suggest that a possible crystallization of the stearic acid domains, promoted by peptide interactions, could be the main responsible of microcapsule irregularities.

DSC was used to evaluate the percentage of shell material in the obtained capsules, based on differences in melting enthalpies. The thermograms of the capsules containing demineralised water (C) and capsules containing 1 % peptide solution (Cp) depicted one main sharp endothermic transition at T_{peak} (°C) of 65.65±0.14 and 64.80±0.04, respectively (Fig. 3a), with corresponding ΔH (J/g) of 19.9±6.3 for C and 22.4±4.7 for Cp. Considering that the ΔH (J/g) of the shell material (75 % stearic acid+25 % carnauba wax), which appeared at the T_{peak} (°C) of 74.21±0.2, was 226.7±0.71 J/g (data not shown), it was deduced that the shell material represented 8.8±3.0 % and 9.9±2.1 % of the total microcapsule weight in C and Cp microcapsules, respectively.

Peptide encapsulation efficiency was 84.7±3.4 %. Encapsulation efficiency in microcapsules is very important in order

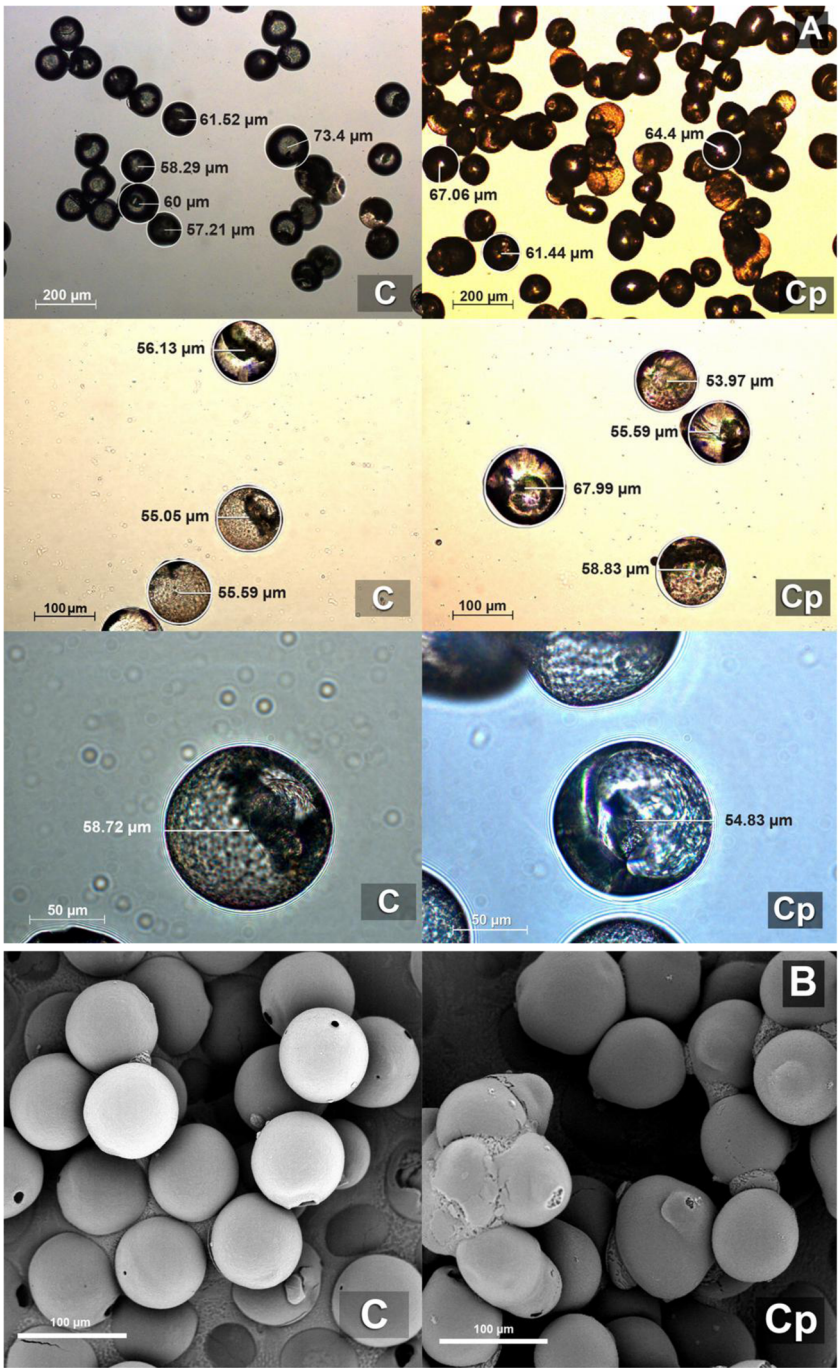

Fig. 2 Optical microscopy (**a**) images and low-temperature scanning electron microscopy (**b**) of C and Cp microcapsules

to study the effectiveness of the process. The obtained peptide content was slightly lower than the targeted concentration, which might be caused by different reasons such as, a lower final peptide concentration in the printed droplet due to minor losses during sample process into the encapsulation printer; a minor loss of the core material's boundary layer suffered from the impact point between the droplet and the screen shell material; or the partial peptide–lipid shell material bonding, which would have not allowed total peptide release. The use of carnauba wax for lipid-based encapsulation materials development has also previously shown more than 80 % of encapsulation efficiency (Bhoyar et al. 2011). Taking into account both the percentage of shell material and the efficiency of encapsulated peptide on dry basis, it could be concluded that the ratio of shell material to peptide was 13.3:1.

Laser scattering analysis (Fig. 4) revealed, with an error lower than 5 %, that *C* had a diameter of d_{90}=122.50 µm, d_{50}=76.82 µm and d_{10}=28.06 µm, while Cp had a diameter of d_{90}=125.83 µm, d_{50}=77.63 µm and d_{10}=30.11 µm. The amount of particles with size lower than 30 µm, not observed

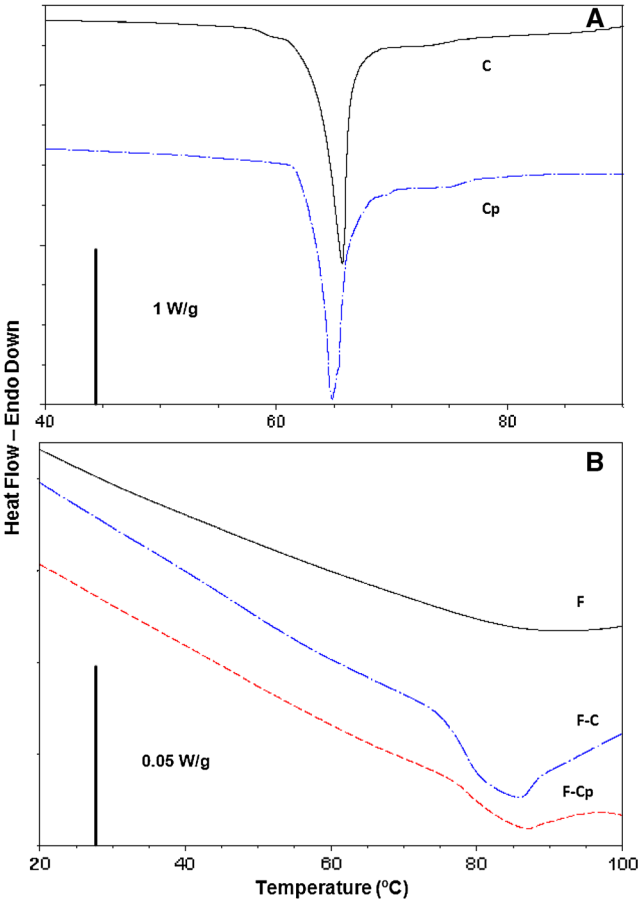

Fig. 3 A. DSC of demineralized water microcapsules (C) and 1 % peptide microcapsules (Cp). B. DSC films (F, F-C and F- Cp)

in microscopic analysis, might be particles of shell material collected from the collision of the encapsulated material with the shell material and/or fragments derived from the sample handling.

Microcapsule Stability at Different pH

Microcapsules are largely meant for incorporation of active ingredients in food products (Mellema et al. 2006). Stability of microcapsules in food systems can be very different depending on a number of environmental factors, including temperature, pH, and moisture content. This study, performed at room temperature (21±1°C), was focussed on the stability of microcapsules subjected to pH variations in aqueous solutions, as a model system mimicking a film forming solution or even high-moisture food products. A high stability would increase the versatility for use of microcapsules in different food systems and processes, including edible films development.

Microcapsule stability profile (Fig. 5) showed that there was an early peptide amount (<10 %) released, which according to Shahidi and Han (1993) could probably be due to residual process inefficiency or some microcapsule breakage. Microcapsules were significantly affected by the environmental pH. Peptide release at pH 2.6 and pH 9.2 was considerably higher than at milder pHs, representing around 40 % of the total peptide content within the first hour. Further release up to 50 % after 3 h was observed at pH 9.2. Microcapsules at pH 5 showed more delayed and progressive release in water, up to around 25 % after 3 h, which might lead to a controlled release model. In this case, no peptides were released during the first hour. At pH 7, peptide release after 3 h was in the same range as at pH 5, but most of the peptide content was released within the first hour.

Carnauba wax coated microcapsules were already reported to be insoluble in water, with release data lower than 30 % during 7 h (Raghuvanshi et al. 1992). Thus, the presence of carnauba wax contributes to slowing down the diffusion of active ingredients through the encapsulation material (Shahidi and Han 1993), although in combination with the stearic acid it normally results in a more porous matrix (Fini et al. 2011).

One possible food application of microcapsules is their addition into edible films. Free peptides can be added in the formulation of edible films, but they normally produce a negative rheological effect due to their plasticizing effect (Giménez et al. 2009). Excessive peptide interactions with

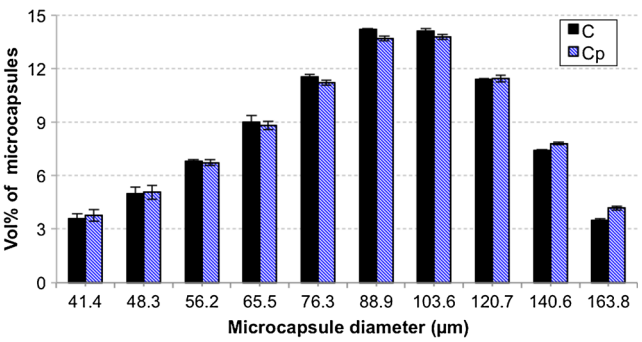

Fig. 4 Microcapsule diameter of C and Cp as determined by laser scattering

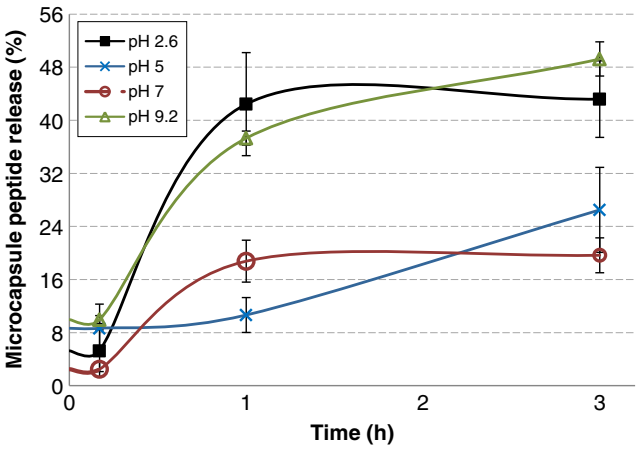

Fig. 5 Microcapsule peptide stability at different pH during the first 3 h at 21°C

matrix components during film preparation can be avoided by peptide microencapsulation, prior to the addition into the filmogenic solution. In the present study, the unrefined seaweed extract was obtained under relatively strong alkaline conditions, therefore, the resulting pH of the alginate-based film forming solution was 10±0.8.

To check microcapsule pH stability upon film drying simulated conditions, kinetics of peptide release were measured at pH 10 and 35°C for 9 h, which is the temperature and maximum time needed for film drying (Fig. 6). For comparison purposes, peptide release was also tested in water at pH 7. No significant differences were observed, showing an early ~30 % release in the first 30 min and being stable thereafter, which was enough to cover the complete drying process. After around 6 h the film dehydration process was completed, ensuring around 70 % of peptides immobilized in the microcapsules in the resulting film. Compared to the pH stability results, temperatures higher than 21°C increased the release rate through the encapsulation matrix, probably due to weakening of the shell material at elevated temperatures and the resulting increased peptide diffusion (Stojaković et al. 2012; Shahidi and Han 1993). Comparing microcapsule stability at pH 7 after 3 h (Figs. 5 and 6), the peptide release was significantly lower at 21°C (~20 %) than at 35°C (~35 %).

Film Preparation

In order to know the relative cohesive and adhesive molecular forces within the filmogenic solution and the added microcapsules, the contact angle (θ) of a droplet of the biopolymeric solution over the shell material was measured, and found to be 100.3±0.9° at 21°C.

The contact angle indicates how hydrophobic the shell material is, where 180º represents absolutely no wetting and smaller contact angles imply increasing hydrophilic surface and higher tendency to wetting. According to Karbowiak et al. (2006), contact angle values θ>65° suggest a predominant hydrophobic system indicating very low surface affinity between the filmogenic solution and the lipid microcapsule surface, which resulted in poor wetting and aggregation of microcapsules, negatively affecting the film forming process. Microcapsule aggregation was resolved by including a surfactant in the formulation of the film forming solution and by immobilization of the well dispersed microcapsules using a porous polycarbonate membrane.

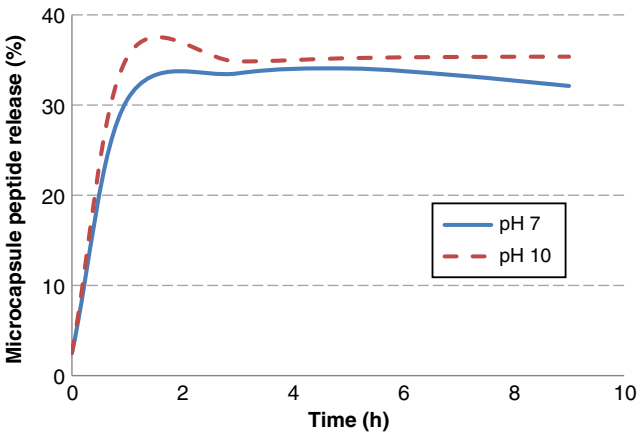

Fig. 6 Microcapsule peptide stability in distilled water pH 7 and pH 10 at 35°C during 9 h

Three different sets of films were prepared: F-C, containing water-filled microcapsules C; F-Cp, containing peptide-filled microcapsules Cp, and F, reference films without microcapsules.

Although the behaviour of C and Cp microcapsules when included into the filmogenic solution was essentially the same, slight differences in microcapsules distribution were perceptible in F-C and F-Cp films, as shown in Fig. 7. Panoramic pictures showed that microcapsules in F-C were more visible at the film surface, while F-Cp microcapsules were more integrated inside the matrix, indicating possible differences in microcapsule density or in the degree of interaction with the film matrix components. Interestingly, addition of both types of microcapsules did not significantly modify the film thickness (~141 μm) with respect to the film without microcapsules (139 μm). Moisture content was significantly higher ($P \leq 0.05$) in F (37.1±0.9 %), while no significant differences were found between F-C (31.0±2.1 %) and F-Cp (31.8±2.1 %), attributed to the hydrophobicity of the microcapsule lipid shell material.

Film Properties

Thermal Properties

DSC thermograms of F, F-C and F-Cp films are shown in Fig. 3b. An endothermic transition attributed to the presence of microcapsules was observed in F-C and F-Cp films at 82.88±0.47°C and 86.87±0.28°C, respectively. The corresponding enthalpies, after re-calculation on dry matter basis to avoid water interferences, were 0.88±0.08 J/g for F-C and 1.23±0.26 J/g for F-Cp. Higher melting temperatures were needed to melt the shell material suggesting that microcapsules were efficiently entrapped into the film matrix. Alginates from F-C and F-Cp films might have interacted with the microcapsule components, probably the stearic acid with more capacity to form interactions. Apparently, Laminaria film matrix protected more efficiently Cp than C capsules, which was registered by higher enthalpy values. The 30 % of peptides released during F-Cp film process might have increased film interactions between filmogenic compounds and peptides resulting in a stronger matrix than F-C. Films did not show any glass transition within the temperature range studied, which might be caused by the presence of glycerol. Films

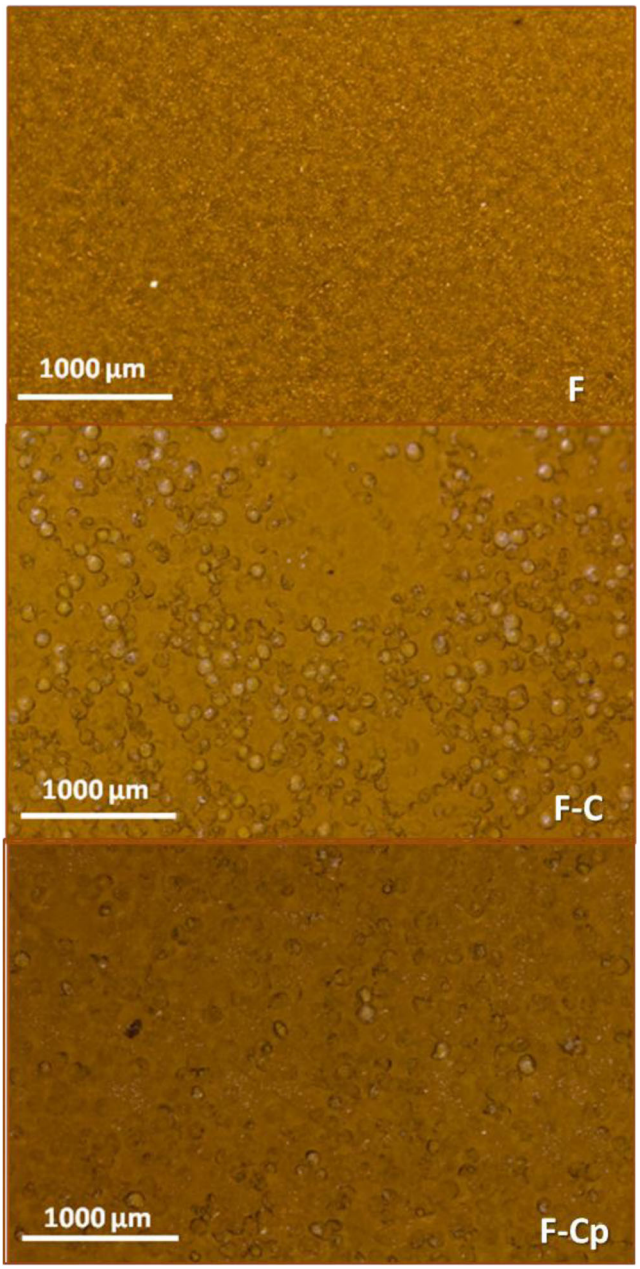

Fig. 7 Panoramic photographic surface images of F, F-C and F-Cp films

made of neat alginates have been reported to be essentially amorphous, with an irregular structure that does not crystallize (Siddaramaiah et al. 2008), and the addition of plasticizer seems to increase that behaviour, probably dropping the glass transition temperatures to a lower range (Avella et al. 2007).

Low-Temperature Scanning Electron Microscopy of F-Cp Film

LT-SEM cross-sectional images of the film containing the Cp microcapsules are shown in Fig. 8. Microcapsules were clearly distinguishable throughout the whole biopolymeric matrix, which exhibited a greatly dense and compact appearance. Capsules mostly retained their structural integrity, but not their spherical morphology. The cross-sectional image shows an empty cavity within the microcapsule, suggesting that the peptide content tends to be disposed inside the wall of the capsule. The inclusion of microcapsules in the films caused a noticeable matrix disruption, in some cases leaving large gaps between the biopolymer and the microcapsules, probably favoured by the strong hydrophobic nature of the shell material. Despite the fact that microcapsules led to strong discontinuities in the film microstructure, the compact nature of the alginate-based matrix was strong enough to support them without being fractured.

Water Barrier Properties

The film water solubility slightly increased ($P \leq 0.05$) with microcapsule incorporation in both F-C and F-Cp (Table 1). The lipid nature of the microcapsule would be expected to reduce film solubility; however microcapsules caused noticeable disruption in the film structure, leading to increased solubility. This effect was contrary to other studies, where lipid content was homogeneously mixed with the principal matrix component during the film forming solution process (Arcan and Yemenicioğlu 2013). Solubility values were much higher than results obtained with commercial alginate films with cation complexation (~5 %) (Pereira et al. 2013), but similar to those developed with sodium alginate without cation complexation (~100 %) (Abdollahi et al. 2013; Zactiti and Kieckbusch 2006). In contrast, F-C and F-Cp showed a significant reduction ($P \leq 0.05$) in the WVP; as compared to the F film (Table 1), which was largely attributed to the hydrophobic nature of the capsule lipid shell material. More specifically, the wax constituent has been previously reported to be effective at reducing the WVP of casein films added with paraffin wax (Sohail et al. 2006) or sodium caseinate–alginate films with beeswax (Fabra et al. 2008). The WVPs of all studied films were considerably higher than previous results obtained with commercial alginate films (Benavides et al. 2012; Tapia et al. 2007), which might be caused by the presence of hydrophilic compounds in the unrefined alginate seaweed extract, such as sulphated polysaccharides, proteins and phenolic compounds (Blanco-Pascual et al., 2014).

Mechanical Properties

F significantly showed the lowest tensile strength (TS), elongation at break (EAB) and elastic Young's modulus (Y) ($P \leq 0.05$) (Table 1), in good accordance to its poorer cross-linked structure. Microcapsule addition considerably increased tensile strength, elongation at break and Young's modulus. Fabra et al. (2008) showed that beeswax addition to sodium caseinate–alginate films improved both elastic modulus and tensile

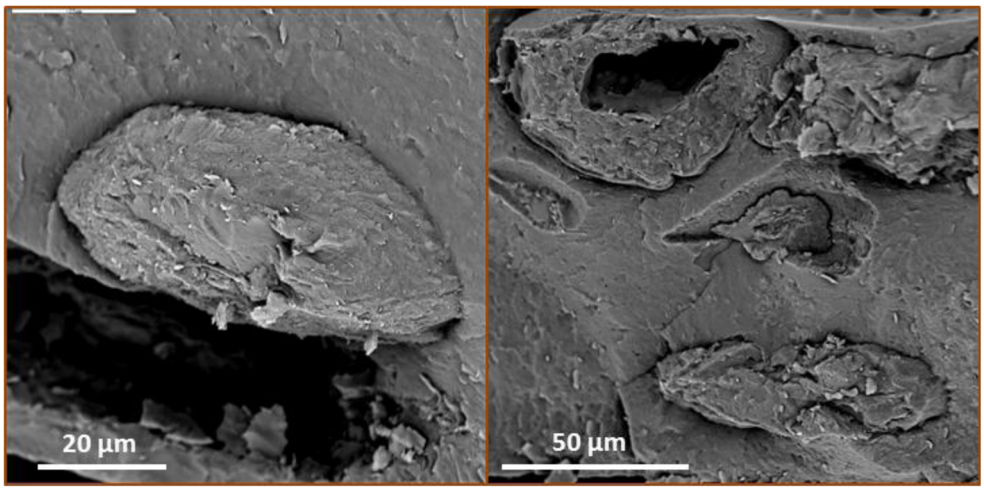

Fig. 8 Low-temperature scanning electron microscopy images of F-Cp cross section

strength but, contrary to our results, reduced elongation at break. EAB and TS values of all studied films were lower than previous films developed with 2–4 % commercial alginate (EAB of 17–30 %) (TS of 12–27 MPa) (Su Cha et al. 2002) and also after adding $CaCl_2$ for cation complexation (~15 % and ~45 MPa) (Pereira et al. 2013).

Regarding puncture deformation (*D*) and force (*F*), microcapsule inclusion in both F-C and F-Cp led to a significant decrease in both *D* and *F* values ($P \leq 0.05$) (Table 1), probably as a result of film matrix disruptions caused by the microcapsules. As in tensile test, no significant differences were found between F-C and F-Cp. Previous results obtained with 1–1.5 % commercial alginate films were in the same *F* range (13–22 N) and *D* range (25–60±3.04 %) as F film (Wang et al. 2007a).

Table 1 Solubility, water vapour permeability (WVP), tensile strength (TS), elongation at break (EAB), Young's modulus (*Y*), puncture force (*F*), puncture deformation (*D*), lightness (L^*), colour values *a**, *b** and transparency ($-\log(T_{600}/x)$) of F, F-C and F-Cp films

Film	F	F-C	F-Cp
Solubility (%)	86.0±1.7 a	94.8±2.9 b	92.9±1.9 b
WVP ($\times 10^{-7}$ g m^{-1} s^{-1} Pa^{-1})	1.80±0.02 a	0.80±0.0 b	0.89±0.3 b
TS (MPa)	6.6±2.1 a	10.8±0.9 b	10.1±0.8 b
EAB (%)	1.31±0.74 a	2.87±0.4 b	3.23±0.2 b
Y (MPa)	88±25 a	183±10 b	185±14 b
F (N)	13.2±2.3 a	8.61±1.5 b	7.44±1.4 b
D (%)	23.1±4.0 a	10.9±1.2 b	9.33±1.5 b
*L**	25.1±0.5 a	25.1±1.1 ab	26.6±0.8 b
*a**	3.52±0.2 a	3.27±0.5 a	3.75±0.6 a
*b**	4.54±0.5 a	4.57±0.8 a	5.92±1.0 a
Transparency	6.99±0.27 a	8.42±0.34 b	7.97±0.28 b

Results are the mean±standard deviation. Different letters (a, b, c) in the same row indicate significant differences among the different films ($P \leq 0.05$)

Thus, it could be concluded that microcapsules incorporation improved film mechanical tensile response due to the lipid microcapsule strength effect, while negatively affected to the puncture test film behaviour. The microcapsule matrix disruption that negatively affected film solubility might have also been responsible of the puncture breakage. While tensile strength test gives us more general mechanical film information, puncture test concentrates the force in one specific little area, being more affected by the discontinuous structure and poor cohesion between the film matrix and the microcapsules.

Colour Properties

As shown in Table 1, film transparency was significantly ($P \leq 0.05$) lower in films containing microcapsules than in the F film, being largely attributed to the presence of the carnauba wax in the shell material. No significant differences were found between F-C and F-Cp ($P \leq 0.05$). *L** (lightness), *a** (reddish/greenish) and *b** (yellowish/bluish) values are also shown in Table 1, where it is revealed that all films had low lightness (25–27). *a** and *b** did not show significant differences with or without entrapped microcapsules ($P \leq 0.05$). The yellowish-brown colouration of films was mainly attributed to the residual presence of fucoxanthin, a typical pigment in the chloroplasts of brown algae, in the unrefined extract used as film forming material (Ferraces-Casais et al. 2012; Blanco-Pascual et al., 2013).

In general, films were less transparent than those previously obtained with isolated commercial alginate, due to their intense colouration and the presence of the microcapsules; but constituted a better light absorption barrier (Yoo and Krochta 2011; Pereira et al. 2013). Films contained most of the seaweed compounds that remained in Laminaria extract, rendering more opaque films with more red-brown colouration; resulting in low lightness and low yellowness tendency

compared to films developed with commercial alginates (Wang et al. 2007b).

Conclusions

Printing of hydrophobic stearic acid/carnauba core–shell microcapsules resulted in an efficient process for active peptide protection. Microcapsule stability and peptide release rate depended on the environmental pH and temperature, giving the possibility of different applications depending on the final food system. Microcapsule inclusion in hydrophilic *L. digitata* edible film matrix resulted in a discontinuous film with improved WVP, higher film solubility and opacity and poorer puncture response. Given the high peptide entrapment efficiency, this encapsulation methodology can be effective to prevent any plasticizing effect induced by the presence of free peptides in the film. *L. digitata* network, with microcapsules embedded in it, could be used for active and edible film applications, as a carrier for a wide range of molecules apart from peptides.

Acknowledgement This research was supported by the Spanish Ministry of Science and Innovation, I+D+I National Plan, under the project AGL2011-27607 and Xunta de Galicia Sectorial program: PEME I+D E I+D SUMA and gratefully thanks to JAE-Predoc CSIC scholarship.

References

Abdollahi, M., Alboofetileh, M., Rezaei, M., & Behrooz, R. (2013). Comparing physico-mechanical and thermal properties of alginate nanocomposite films reinforced with organic and/or inorganic nanofillers. *Food Hydrocolloids, 32*(2), 416–424.

AOAC (1995). Official methods of analysis. Maryland, USA: Association of Official Analytical Chemistry

Arcan, I., & Yemenicioğlu, A. (2013). Development of flexible zein–wax composite and zein–fatty acid blend films for controlled release of lysozyme. *Food Research International, 51*(1), 208–216.

Avella, M., Pace, E. D., Immirzi, B., Impallomeni, G., Malinconico, M., & Santagata, G. (2007). Addition of glycerol plasticizer to seaweeds derived alginates: Influence of microstructure on chemical–physical properties. *Carbohydrate Polymers, 69*(3), 503–511.

Balducci, A. G., Colombo, G., Corace, G., Cavallari, C., Rodriguez, L., Buttini, F., Colombo, P., & Rossi, A. (2011). Layered lipid microcapsules for mesalazine delayed-release in children. *International Journal of Pharmaceutics, 421*(2), 293–300.

Benavides, S., Villalobos-Carvajal, R., & Reyes, J. E. (2012). Physical, mechanical and antibacterial properties of alginate film: effect of the crosslinking degree and oregano essential oil concentration. *Journal of Food Engineering, 110*(2), 232–239.

Bhoyar, P. K., Morani, D. O., Biyani, D. M., Umekar, M. J., Mahure, J. G., & Amgaonkar, Y. M. (2011). Encapsulation of naproxen in lipid-based matrix microspheres: characterization and release kinetics. *Journal of Young Pharmacists, 3*(2), 105–111.

Blanco-Pascual, N., Fernández-Martín, F., & Montero, M. P. (2013). Effect of different protein extracts from *Dosidicus gigas* muscle co-products on edible films development. *Food Hydrocolloids, 33*(1), 118–131.

Blanco-Pascual, N., Montero, M. P., & Gómez-Guillén, M. C. (2014). Antioxidant film development from unrefined extracts of brown seaweeds *Laminaria digitata* and *Ascophyllum nodosum*. *Food Hydrocolloids, 37*, 100–110.

de Vos, P., Faas, M. M., Spasojevic, M., & Sikkema, J. (2010). Encapsulation for preservation of functionality and targeted delivery of bioactive food components. *International Dairy Journal, 20*(4), 292–302.

Fabra, M. J., Talens, P., & Chiralt, A. (2008). Effect of alginate and λ-carrageenan on tensile properties and water vapour permeability of sodium caseinate-lipid based films. *Carbohydrate Polymers, 74*(3), 419–426.

Ferraces-Casais, P., Lage-Yusty, M. A., de Quirós, A. R., & López-Hernández, J. (2012). Evaluation of bioactive compounds in fresh edible seaweeds. *Food Analytical Methods, 5*(4), 828–834.

Fini, A., Cavallari, C., Rabasco Alvarez, A. M., & Rodriguez, M. G. (2011). Diclofenac salts: Part 6. Release from lipid microspheres. *Journal of Pharmaceutical Sciences, 100*(8), 3482–3494.

Gibbs, B. F., Kermasha, S., Alli, I., & Mulligan, C. N. (1999). Encapsulation in the food industry: a review. *International Journal of Food Sciences and Nutrition, 50*(3), 213–224.

Giménez, B., Gómez-Estaca, J., Alemán, A., Gómez-Guillén, M. C., & Montero, M. P. (2009). Improvement of the antioxidant properties of squid skin gelatin films by the addition of hydrolysates from squid gelatin. *Food Hydrocolloids, 23*(5), 1322–1327.

Gómez-Guillén, M. C., Ihl, M., Bifani, V., Silva, A., & Montero, P. (2007). Edible films made from tuna-fish gelatin with antioxidant extracts of two different murta ecotypes leaves (*Ugni molinae* Turcz). *Food Hydrocolloids, 21*(7), 1133–1143.

Goodwin, D., Simerska, P., & Toth, I. (2012). Peptides as therapeutics with enhanced bioactivity. *Current Medicinal Chemistry, 19*(26), 4451–4461.

Gouin, S. (2004). Microencapsulation: industrial appraisal of existing technologies and trends. *Trends in Food Science & Technology, 15*, 330–347.

Houben RJ (2012) Equipment for printing of high viscosity liquids and molten metals. Doctoral thesis, University of Twente, The Netherlands

Joseph, I., & Venkataram, S. (1995). Indomethacin sustained release from alginate-gelatin or pectin-gelatin coacervates. *International Journal of Pharmaceutics, 126*(1–2), 161–168.

Karbowiak, T., Debeaufort, F., Champion, D., & Voilley, A. (2006). Wetting properties at the surface of iota-carrageenan-based edible films. *Journal of Colloid and Interface Science, 294*(2), 400–410.

Koldeweij RBJ (2010). Encapsulation of micron sized droplets. MSc thesis, University of Twente, The Netherlands

Krochta, J. M., & DeMulderJohnston, C. (1997). Edible and biodegradable polymer films: challenges and opportunities. *Food Technology, 51*(2), 61–74.

Mellema, M., Van Benthum, W. A. J., Boer, B., Von Harras, J., & Visser, A. (2006). Wax encapsulation of water-soluble compounds for application in foods. *Journal of Microencapsulation, 23*(7), 729–740.

Mosquera M, Giménez B, Ramos S, López-Caballero ME, Gómez-Guillén MC & Montero P (2013). Antioxidant, ACE-inhibitory and antimicrobial activities of peptide fractions obtained from dried giant squid tunics. Journal of Aquatic Food Product Technology, in press

Pereira, R., Carvalho, A., Vaz, D. C., Gil, M. H., Mendes, A., & Bártolo, P. (2013). Development of novel alginate based hydrogel films for wound healing applications. *International Journal of Biological Macromolecules, 52*(1), 221–230.

Perez-Mateos, M., Montero, P., & Gomez-Guillen, M. C. (2009). Formulation and stability of biodegradable films made from cod gelatin and sunflower oil blends. *Food Hydrocolloids, 23*(1), 53–61.

Raghuvanshi, R. S., Tripathi, K. P., Jayaswal, S. B., & Singh, J. (1992). Release kinetics of salbutamol sulphate from wax coated

microcapsules and tableted microcapsules. *Journal of Microencapsulation, 9*(4), 449–456.

Shahidi, F., & Han, X. Q. (1993). Encapsulation of food ingredients. *Critical Reviews in food Science and Nutrition, 33*(6), 501–547.

Siddaramaiah, Swamy, T. M. M., Ramaraj, B., & Lee, J. H. (2008). Sodium alginate and its blends with starch: thermal and morphological properties. *Journal of Applied Polymer Science, 109*(6), 4075–4081.

Sobral, P. J. A., Menegalli, F. C., Hubinger, M. D., & Roques, M. A. (2001). Mechanical, water vapor barrier and thermal properties of gelatin based edible films. *Food Hydrocolloids, 15*(4–6), 423–432.

Sohail, S. S., Wang, B., Biswas, M. A. S., & Oh, J. H. (2006). Physical, morphological, and barrier properties of edible casein films with wax applications. *Journal of Food Science, 71*(4), 255–259.

Stojaković, D., Bugarski, B., & Rajić, N. (2012). A kinetic study of the release of vanillin encapsulated in *Carnauba wax* microcapsules. *Journal of Food Engineering, 109*(3), 640–642.

Su Cha, D., Choi, J. H., Chinnan, M. S., & Park, H. J. (2002). Antimicrobial films based on Na-alginate and κ-carrageenan. *LWT - Food Science and Technology, 35*(8), 715–719.

Sun-Waterhouse, D., & Wadhwa, S. S. (2013). Industry-relevant approaches for minimising the bitterness of bioactive compounds in functional foods: a review. *Food and Bioprocess Technology, 6*(3), 607–627.

Tapia, M. S., Rojas-Graü, M. A., Rodríguez, F. J., Ramírez, J., Carmona, A., & Martin-Belloso, O. (2007). Alginate- and gellan-based edible films for probiotic coatings on fresh-cut fruits. *Journal of Food Science, 72*(4), 190–196.

Tomaszewski, J. E., Schwarzenbach, R. P., & Sander, M. (2011). Protein encapsulation by humic substances. *Environmental Science and Technology, 45*(14), 6003–6010.

Wang, B., Jia, D. Y., Ruan, S. Q., & Qin, S. (2007a). Structure and properties of collagen–konjac glucomannan–sodium alginate blend films. *Journal of Applied Polymer Science, 106*(1), 327–332.

Wang, L. Z., Liu, L., Holmes, J., Kerry, J. F., & Kerry, J. P. (2007b). Assessment of film-forming potential and properties of protein and polysaccharide-based biopolymer films. *International Journal of Food Science and Technology, 42*(9), 1128–1138.

Yoo, S., & Krochta, J. M. (2011). Whey protein-polysaccharide blended edible film formation and barrier, tensile, thermal and transparency properties. *Journal of the Science of Food and Agriculture, 91*(14), 2628–2636.

Zactiti, E. M., & Kieckbusch, T. G. (2006). Potassium sorbate permeability in biodegradable alginate films: effect of the antimicrobial agent concentration and crosslinking degree. *Journal of Food Engineering, 77*(3), 462–467.

Zadmard, R., & Schrader, T. (2004). Nanomolar protein sensing with embedded receptor molecules. *Journal of the American Chemical Society, 127*(3), 904–915.